

Functional diversity of R3 single-repeat genes in trichome development

Katja Wester¹, Simona Digiuni¹, Florian Geier², Jens Timmer³, Christian Fleck³ and Martin Hülskamp^{1,*}

Trichome and root hair patterning are governed by a conserved cassette of bHLH and MYB factors, the WD40 protein TTG1, and six single-repeat MYB R3 factors that are thought to counteract them. In this work we focus on the single-repeat R3 factor ETC3 and show that its major role is in the regulation of trichome density in a redundant manner. Diversification of the *ETC3* gene has occurred at the promoter level, as *etc3* mutants can be rescued by expressing ETC3 under the control of the *TRY* or *CPC* promoter. ETC3 movement was detected between epidermal cells as well as between the epidermis and underlying tissues. Finally, we found marked differences in the ability of the single-repeat R3 factors to interfere with the dimerisation of GL1 and GL3 in a yeast three-hybrid system, with CPC being the most potent inhibitor followed by ETC1, TRY, ETC3 and ETC2. Mathematical analysis predicts that this behaviour has a major impact on protein mobility, suggesting a tight reverse correlation between inhibitory function and the diffusion/transport range of the inhibitors. This prediction is supported by a comparison of CPC and ETC3 mobility in *egl3 gl3* double mutants and 35S:GL3 lines.

KEY WORDS: Trichomes, Patterning, *Arabidopsis*

INTRODUCTION

The differentiation of epidermal cell types in a spatially regulated manner is an excellent model system in which to study pattern formation in plants. Two apparently independent patterning systems have been recognised: one that controls the spatial distribution of stomata (Bergmann and Sack, 2007; Serna, 2005) and one that controls the spatial distribution of root hairs and trichomes on leaves (Ishida et al., 2008; Larkin et al., 2003; Pesch and Hülskamp, 2004; Schellmann et al., 2007). The latter patterning system is based on an evolutionarily conserved gene cassette consisting of three types of positive regulators comprising a WD40 protein, R2R3 MYB-type transcription factors and bHLH transcription factors, and negative regulators of the single-repeat R3 MYB transcription factor family. The WD40 protein is encoded by the single-copy gene *TRANSPARENT TESTA GLABRA1 (TTG1)* (Galway et al., 1994; Walker et al., 1999). The R2R3 MYB-type transcription factors are represented by a small gene family, with *GLABRA1* and *MYB23* functioning in trichome patterning and *WEREWOLF* in root hair patterning (Kirik et al., 2005; Kirik et al., 2001; Lee and Schiefelbein, 1999; Oppenheimer et al., 1991). The bHLH factors are *GLABRA3* and *ENHANCER OF GLABRA3 (EGL3)*, which act redundantly in trichome and root hair patterning (Bernhardt et al., 2005; Payne et al., 2000; Zhang et al., 2003). The single-repeat R3 MYB proteins act as negative regulators and have been grouped into a family of six genes (Wang et al., 2007). The *CAPRICE (CPC)* gene was initially identified as a major regulator of root hair development, whereas *TRIPTYCHON (TRY)* is predominantly required for trichome patterning (Kirik et al., 2004a; Kirik et al., 2004b; Schellmann et al., 2007; Wada et al., 1997). Subsequent analysis showed that *CPC* and *TRY* act redundantly in root hair and trichome development (Schellmann et al., 2007). Also, two other members of

the family, *ENHANCER OF TRY AND CPC 1 (ETC1)* and *ETC2*, act redundantly with *TRY* and *CPC* (Esch et al., 2004; Kirik et al., 2004a; Kirik et al., 2004b). In addition, *TRICHOMELESS1 (TCL1)* has been shown to play an important role in trichome formation on the stem and the pedicels (Wang et al., 2007). In an initial report, the analysis of *etc3* mutants focused on root hair development (Simon et al., 2007). More recently, further phenotypes caused by mutations in *ETC3* were studied and *CPL3 (CPC-LIKE-MYB3)* was introduced as a second name for this gene (Tominaga et al., 2008). *ETC3* seems to represent an unusual member of the single-repeat R3 MYB class, as various unusual phenotypes were reported for the mutant including an early flowering time phenotype, reduced trichome size and branching, longer hypocotyls and general plant growth changes (Tominaga et al., 2008). A role for ETC3 in trichome formation is controversial. Tominaga and co-workers reported a higher trichome density in the corresponding mutant and, in contrast to the other members of the single-repeat R3 MYBs, a conspicuous absence of trichome-specific expression (Tominaga et al., 2008). Wang and co-workers could not detect any difference in trichome number between *etc3* single mutants and the corresponding wild type (Wang et al., 2008).

The positive regulators are thought to form a complex in which the R2R3 MYB factor and TTG1 bind to GL3 or EGL3, and the negative regulation by the R3 single-repeat MYBs is postulated to be governed by their competition with MYB factors for binding to GL3 and EGL3, thereby rendering the activator complex inactive (Bernhardt et al., 2003; Esch et al., 2003; Payne et al., 2000). Inhibition by direct binding to the *GL1* promoter was suggested by ChIP experiments for *TCL1* (Wang et al., 2007).

Although the same machinery is central to the spatial regulation of root hair and trichome patterning, the context is different. Whereas trichome formation on rosette leaves takes place without a recognisable reference to other leaf structures except for other trichomes (Hülskamp and Schnittger, 1998; Larkin et al., 1996), root hair patterning is strongly biased such that root hairs are normally found only in epidermal cells overlying a cleft between two underlying cortex cells (Berger et al., 1998; Dolan et al., 1994). For both systems, models that try to explain pattern formation are based on a feedback loop in which the positive regulators activate the

¹University of Cologne, Botanical Institute III, Gyrhofstr. 15, 50931 Cologne, Germany. ²University of Freiburg, Department of Biology, Schaezenlestr. 1, 79104 Freiburg, Germany. ³University of Freiburg, Department of Mathematics and Physics, Hermann-Herder-Str. 3a, 79104 Freiburg, Germany.

*Author for correspondence (e-mail: martin.huelskamp@uni-koeln.de)

negative regulators and the negative regulators inhibit the activators, with the negative regulators being able to move between cells (Digijuni et al., 2008; Larkin et al., 1996; Marks and Esch, 2003; Pesch and Hulskamp, 2004; Scheres, 2002). Recently, evidence for a parallel second patterning system has been reported in which the depletion of TTG1 around incipient trichomes contributes to pattern formation (Bouyer et al., 2008).

In this study we focus on the function of the single-repeat R3 MYB factors in trichome patterning with emphasis on ETC3. Initially, we reassess the published molecular and genetic data (Tominaga et al., 2008; Wang et al., 2008). We show that *ETC3* is expressed in trichomes, that trichome density is increased in *etc3* mutants and that this phenotype can be rescued by a pETC3:ETC3 construct. Our data do not support most of the additional phenotypes, such as the flowering time, the hypocotyl length and the trichome size and branching phenotypes previously reported. Next, we compared the molecular function of TRY, CPC, ETC1, ETC2 and ETC3. These factors differ in their binding strength to GL3 and, using the yeast three-hybrid system, we show that their capacity to compete with GL1 for binding to GL3 also differs. Marked differences were found, with CPC being the most potent inhibitor followed by ETC1, TRY, ETC3 and ETC2. We further show that ETC3 protein can travel between cells. Promoter-swap experiments revealed that transcriptional regulation, in particular, is important for the functional diversity. Mathematical analysis suggests that the mobility of the inhibitors depends on their affinity for GL3. This prediction is supported by a comparison of the mobility of CPC and ETC3 in *egl3 gl3* double mutants and 35S:GL3 lines.

MATERIALS AND METHODS

Plant material and growth conditions

The following single and double mutants were used in this study and have been described previously: *cpc-1* in WS ecotype (Wada et al., 1997), *try-82* in *Ler* ecotype (Hulskamp et al., 1994), *try-JC* in Col ecotype (Larkin et al., 1999), *etc1* in Col ecotype (Kirik et al., 2004a), *etc2* in WS ecotype (Kirik et al., 2004b), *etc3* in Col ecotype (Simon et al., 2007) and *cpc try* double mutant (Schellmann et al., 2002). Plants homozygous for multiple mutations were constructed by crossing single, double or triple mutants. The single and multiple mutants were confirmed by PCR. All MS plates contained 1% sucrose. The *gl3 egl3* double mutant was created by crossing the single mutants *gl3* (Salk_118201) and *egl3* (Salk_019114). The GL3-overexpressing line was established by transformation of wild-type (Col) plants with the pAM-PAT p35S:GL3 construct.

Agrobacterium-mediated transformation of *Arabidopsis* plants was performed as described (Clough and Bent, 1998).

Cytological methods

GUS staining using X-glucuronide was performed as described (Vroemen et al., 1996). Fourteen-day-old plants from soil were used for GUS staining of leaves. The root expression analysis was performed with 5-day-old plants grown on MS plates. Pictures were taken with a light microscope equipped with DISKUS software (Carl H. Hilgers-Technisches Büro, Königswinter, Germany; version 4.30.19).

For staining cell walls, a propidium iodide solution (0.3 mg/ml) was used. Plant material was incubated for 5 minutes at room temperature and washed twice in water.

Evaluation of root-hair numbers and stomata density

For quantification of root hairs, plants were grown on MS plates in a vertical orientation for 5 days. Stomata numbers were determined on 3-week-old leaves stained with propidium iodide. Using a confocal laser-scanning microscope, a 1 mm² area of the fourth leaf was scanned for the statistical analysis.

Confocal laser-scanning microscopy (CLSM)

For CLSM, a Leica SP2 was used. Pictures were taken using the LCS software and images processed using Adobe Photoshop 6.0.

The quantitative comparison of YFP signals in neighbouring cells was based on full stacks that were subsequently merged to one plane. The resulting raw image was analysed using Leica Confocal Histogram Quantification software. In order to determine how much signal of the initially targeted cell arrives in the neighbouring cell, the signal intensity of the nuclei was compared.

Nucleic acid analysis

Plants carrying the T-DNA insertion in the *ETC3* gene were identified by PCR on genomic DNA using primers ETC3-for (5'-ATGGATAACCATC-GCAGGAC-3') and LBa1 (5'-TGGTTCACGTAGTGGGCCATCG-3').

ETC3 cDNA was amplified from Col wild-type cDNA by PCR using primers ETC3-XbaI-for (*XbaI* site added, 5'-TCTAGAATGGATAAC-CATCGCAGGAC-3'), ETC3-SacI-rev (*SacI* site added, 5'-GAGCTCT-CAATTTTCATGACCCAA-3'). The PCR product was subcloned into pBluescript (pBS) with 5' *XbaI* and 3' *SacI* restriction sites downstream of GFP cDNA.

The *ETC3* cDNA in pBS was amplified by PCR using primers ETC3-attB1 (5'-GGGGACAAGTTTGTACAAAAAAGCAGGCTTGATGGAT-AACCATCGCAGGACTAAGCA-3') and ETC3-attB2 (5'-GGGGACC-ACTTTGTACAAGAAAGCTGGGTCTCAATTTTCATGACCCAAA-ACCTC-3'). The PCR product was recombined in the DONR201 vector by the BP reaction (Invitrogen) and constitutes the ETC3 pEntry clone.

The GFP-ETC3 fusion fragment was amplified and recombined through BP in pDONR201 using primers GFP-attB1 (5'-GGGGACAAGTTTGTACAAAAAAGCAGGCTTGATGGTGAGCAAGGGCGAGGAGCT-GT-3') and ETC3-attB2. The YFP-ETC3 pEntry was created by exchanging the GFP for YFP in the entry clone.

A 2023 bp fragment upstream of the *ETC3* start codon was used as the putative 5' *ETC3* promoter. The promoter fragment was amplified by PCR from genomic Col DNA using primers 5'-pETC3-for (5'-ATTCTG-GATTCCTATACATAAC-3') and 5'-pETC3-rev (5'-GTCAAACG-GCACCGTATTAC-3'). The PCR product was subcloned into *SmaI*-cut pBS by blunt-end ligation. The promoter was cloned into the pAM-PAT-GW p35S vector (GenBank AY436765) with 5' *Ecl136II/AscI* (blunt) and 3' *XhoI* restriction sites, resulting in an exchange of the 35S promoter for the *ETC3* promoter. For the *CPC* promoter, a 1091 bp fragment upstream of the start codon was used. For the *TRY* promoter, a 1.4 kb fragment upstream of the *TRY* start codon was used (Schellmann et al., 2002). Both fragments were cloned into the pAM-PAT-GW vector, exchanging the *CPC* or *TRY* for the 35S promoter.

The *RUBISCO SMALL SUBUNIT 2B (RBCS-2B)* promoter (pRbcS2b) was cloned from the pK1573 plasmid (gift from the David Jackson laboratory, Cold Spring Harbor, NY, USA) into the pAM-PAT-GW vector, exchanging for the 35S promoter.

ETC3/GFP-ETC3/YFP-ETC3 entry clones were recombined in the p35S pAM-PAT, 5'pETC3 pAM-PAT, 5'pTRY pAM-PAT or 5'CPC pAM-PAT vector by the LR reaction (Invitrogen).

The p35S:YFP-CPC construct was cloned by the LR reaction. The CPC entry clone was recombined in the 5'YFPpENS vector.

The GFP-ER tag cDNA was amplified from a subclone by PCR using primers GFP-ER-attB1 (5'-GGGGACAAGTTTGTACAAAAAAGC-AGGCTTGATGAAGACTAATCTTTTCTCTTTTCAT-3') and GFP-ER-attB2 (5'-GGGGACCACTTTGTACAAGAAAGCTGGGTCTTAA-AGTTCATCATGTTT-3'). The PCR product was cloned in pDONR201 by the BP reaction and recombined in the 5'pETC3 pAM-PAT vector.

For RT-PCR of full-length cDNA, the *ETC3*-specific primers *ETC3*-for and *ETC3*-rev (5'-CAATTTTCATGACCCAAA-3') were used. For amplification of the first and second exons, *ETC3.1*-for (5'-ATGGATAAC-CATCGCAGGAC-3') and *ETC3.2*-rev (5'-ATGCATTCGAGAGAC-CAAAT-3') were used. Actin primers served as control for DNA content: Actin-for (5'-TGCGACAATGGAAGTGAATG-3') and Actin-rev (5'-GGATAGCATGTGGAAGTGCATAC-3').

BiFC method in protoplasts

The pBATL vectors pCL112 YFP N-term and pCL113 YFP C-term (gift of Sean Chapman, SCRI, Dundee, UK) were used. GL3 and GL3-Δ1-96 [truncated GL3 (Payne et al., 2000)] were fused with the YFP N-term, and

ETC1, ETC2, ETC3, CPC and TRY with the YFP C-term vector. Protoplast isolation and transfection were performed as described (Spitzer et al., 2006).

Yeast two-hybrid and three-hybrid assays

All assays were performed in the *Saccharomyces cerevisiae* strain AH109. Transformation was performed as described (Gietz and Schiestl, 1995). For two-hybrid assays, the GAL4 DNA-BD plasmid pAS2-1 and GAL4 DNA-AD plasmid pAct from Clontech were used. GL3 was fused to the DNA-AD in pACT. GL1Δ (lacking 27 amino acids at the C-terminus), ETC1, ETC2, ETC3, CPC and TRY were fused to the DNA-BD in pAS. For analysing protein-protein interactions, yeasts were grown on media lacking histidine and supplemented with 5 mM 3-amino-1, 2, 4-triazole.

For three-hybrid assays, GL3 was fused to the DNA-AD in pAct. GL1Δ was fused to the GAL4 DNA-BD in the pBridge vector (Clontech). ETC1, ETC2, ETC3, CPC and TRY were fused downstream of the methionine-repressible promoter in pBridge. For analyzing competition between GL1 and one of the other inhibitor proteins for binding to GL3, yeasts were grown on plates lacking histidine. The plates contained different concentrations of methionine (0, 100, 250 or 500 μM) and were supplemented with 50 mM 3-amino-1, 2, 4-triazole.

Transient expression

Rosette leaves were co-bombarded with DNA-coated gold particles using the Biolistic PDS-1000/He system (Bio-Rad). Gold particles (1.0 μm) were coated with 400 ng of each DNA. Particles were bombarded into epidermal cells of rosette leaves with 900-psi rupture disks under a vacuum of 26 inches of Hg. The p35S:YFP-peroxisome (PTS) construct was used as a marker to identify the transformed cells (Mathur et al., 2002). The fluorescence analysis was carried out 7-15 hours later.

Mathematical modelling

The effect of depletion on the mobility of the inhibitors was studied by mathematical modelling. The inhibitor U is produced from a point source (the targeted cell) with a rate κ . It diffuses into the tissue with a rate constant D and is degraded with a rate constant λ . U is also depleted by an irreversible binding to GL3 (G) with a rate constant β . These assumptions lead to the following one-dimensional second-order differential equation for the steady state profile of $U(X)$:

$$D \frac{\partial^2 U(X)}{\partial X^2} = U(X)[\lambda + \beta G(X)], \quad (1a)$$

$$D \frac{\partial U(0)}{\partial X} = -\kappa, \quad (1b)$$

$$U(\infty) = 0. \quad (1c)$$

The production of U is stated in the boundary condition 1b. Boundary condition 1c ensures that the profile of U declines to zero for $X \rightarrow \infty$, as the source of U at $X=0$ is the only source in the considered domain. In the following we assume that GL3 is spatially uniform, i.e. $G(X)=\text{constant}$. The movement ability of the inhibitor is measured by its characteristic decay length (CDL), α , which is the distance from the source at which the inhibitor level drops to $1/e$ (37%) of its source level. We use a scaling approach in order to identify the effective parameters of the problem. The following substitutions for the concentrations U and G and the spatial coordinate X are introduced:

$$u = U \frac{D}{\alpha_0 \lambda}, \quad g = G \frac{D}{\alpha_0 \beta}, \quad x = X \alpha_0^{-1}.$$

The factor $\alpha_0 = \sqrt{D/\lambda}$ is the CDL of U for $\beta=0$. Using these substitutions gives the new dimensionless system:

$$\frac{\partial^2 u(x)}{\partial x^2} = u(x) \left[1 + \frac{\alpha_0 \beta}{D} g \right], \quad (2a)$$

$$\frac{\partial u(0)}{\partial x} = -\kappa / \lambda, \quad (2b)$$

$$U(\infty) = 0. \quad (2c)$$

The solution of equation 2 is $u(x) = c \exp(-x/\sqrt{1+\gamma})$ where $c = \kappa/(\lambda\sqrt{1+\gamma})$ and $\gamma = (\alpha_0 \beta g)$ are the only effective parameters of the problem. Parameter γ has a convenient interpretation because it is the ratio of two time scales: the time it takes one unit of u to diffuse a distance of α_0 and the time it takes one unit of u to bind to one unit of g . The parameter γ can be interpreted as a measure for the relative binding affinity of u for g . The relative CDL of the inhibitor as plotted in the inset of Fig. 5 is given by $\alpha/\alpha_0 = 1/\sqrt{1+\gamma}$.

RESULTS

Isolation of the *etc3* mutant

The *ETC3* gene is the smallest of the six-member R3-type MYB-domain *TRY/CPC*-like gene group (Simon et al., 2007; Tominaga et al., 2008). The deduced 75-amino-acid ETC3 protein shows high homology to TRY and CPC (38% and 50% amino acid identity, respectively). Our comparison of the genomic and cDNA sequences showed that the *ETC3* gene consists of three exons and two introns (Fig. 1A).

As a first step towards a functional analysis of the *ETC3* gene, we isolated a T-DNA knockout line of the corresponding *At4G01060* locus. The SALK line 094027 has an insertion after 354 bp in the second intron (Fig. 1A). RT-PCR analysis with primers in exons 1 and 2 before the insertion yielded no amplification product, indicating that the isolated mutant is a null (Fig. 1B).

We noticed that *etc3* mutant plants exhibit a higher trichome density. On leaves one and two, as well as on leaves three and four, ~50% more trichomes were found as compared with the respective Columbia wild-type background (Table 1; Fig. 2A,B). In order to ensure that this phenotype is due to a mutation in the *ETC3* gene, we expressed the *ETC3* cDNA under the control of a 2023 bp upstream putative promoter fragment. This pETC3:ETC3 construct rescued the trichome phenotype completely (Table 1).

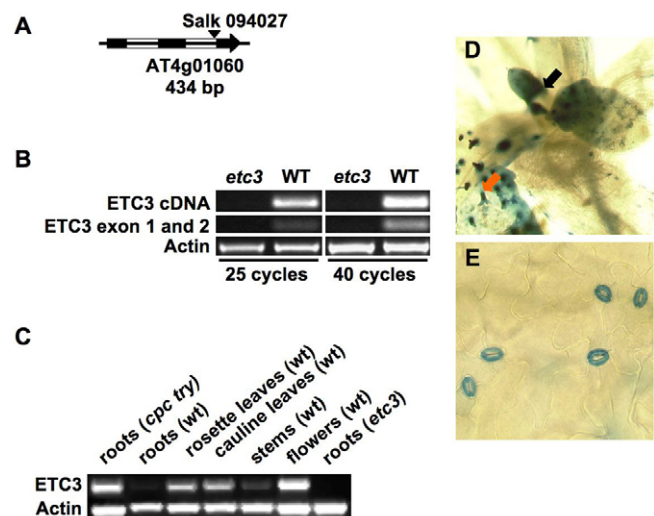


Fig. 1. Molecular and cytological expression analysis of

***Arabidopsis ETC3*.** (A) The *ETC3* gene. Exons, black; introns, white. The T-DNA insertion of the salk line 094027 is located in the second intron (arrowhead). (B) RT-PCR of *etc3* and wild type (WT) using primers that amplify full-length *ETC3* cDNA or only the first two exons. Actin serves as a control. (C) RT-PCR of different tissues in WT and in *cpc try* plants to analyse the transcription level of *ETC3* (30 cycles). Root material from *etc3* was included to demonstrate the specificity of the primers. (D) GUS reporter expression from the *ETC3* promoter in rosette leaves. The basal expression is indicated with a black arrow. The orange arrow indicates trichome-specific expression. (E) *ETC3* promoter-driven GUS reporter expression in the stomata of older leaves.

Table 1. Trichome density on rosette leaves in *etc3* mutants and in *ETC3* overexpression lines

Genotype	Number of trichomes per leaf	
	First leaf pair	Second leaf pair
WT (Col)	16.6±2.2	45.5±7.2
<i>etc3</i> (Col)	25.6±2.9	71.0±10.4
p35S: <i>ETC3</i>	0±0	0±0
5'p <i>ETC3</i> : <i>ETC3 etc3</i>	11.5±4.0	44.9±14.6
5'pCPC: <i>ETC3 etc3</i>	11.4±2.8	46.7±14.0
5'pTRY: <i>ETC3 etc3</i>	12.5±3.1	48.2±13.7
pRbcS: <i>ETC3</i>	5.4±2.8	20.5±8.6
pRbcS:CPC	3.9±3.0	16.9±8.2

For each line, leaf pairs from 45 plants were examined.
WT, wild type.

The expression of *ETC3* was initially studied by RT-PCR. *ETC3* was expressed in all analysed tissues ranging from very weak expression in the root to strong expression in flowers (Fig. 1C). This expression profile generally fits the expression analysis of Tominaga and co-workers (Tominaga et al., 2008). For a better spatial resolution we used the 2023 bp promoter fragment shown to rescue the trichome phenotype to drive the expression of the GUS marker gene (p*ETC3*:GUS). Plant lines containing this construct showed GUS expression in the basal parts of leaves in young trichomes (Fig. 1D) and in stomata (Fig. 1E). Expression ceased during trichome differentiation and was absent in mature trichomes. Because Tominaga and co-workers were unable to detect *ETC3* expression in trichomes (Tominaga et al., 2008), we reasoned that this might be due to differences in the promoter fragments. To test this possibility we created a p*ETC3*:GUS construct using the same 2.4 kb promoter fragment as described by Tominaga et al. (Tominaga et al., 2008). *Arabidopsis* lines containing this construct revealed the same expression pattern as we found for the 2023 bp fragment, including expression in trichomes (see Fig. S1 in the supplementary material).

In roots, p*ETC3*:GUS expression was only occasionally detected after more than 24 hours GUS staining and is therefore not considered further. However, RT-PCR revealed strong expression in *try cpc* double mutants (Fig. 1C). This indicates that *ETC3* is only weakly expressed in roots owing to repression by the other inhibitors, similar to what has been found for *TRY* (Schellmann et al., 2002).

Redundant function of *ETC3* in trichome patterning

To further investigate the role of *ETC3* in trichome patterning we expressed a p35S:*ETC3* construct in a wild-type background. As observed previously for all other members of the *TRY/CPC* group, overexpression of *ETC3* resulted in a glabrous phenotype (Fig. 2C; Table 1).

A potential redundant functional overlap with the other four members of the *TRY/CPC* group was tested by creating double, triple and quadruple mutants (Table 2). As a first step, we compared the four possible double mutants of *etc3* with the *try/cpc* group members. The single mutants fell into three phenotypic classes: *try*, which exhibited trichome clusters; *cpc* and *etc2*, which exhibited increased trichome number; and *etc1*, which was without a detectable trichome phenotype. The *etc3 try* double mutant displayed a weak synergistic phenotype. Trichome density was similar to that of *etc3* mutants and cluster frequency was significantly increased compared with *try* mutants (Student's *t*-test, $P=0.006$). The *cpc etc3* double mutant showed a similar phenotype to the *cpc* single mutant. The *etc3 etc1* double mutant showed a significant increase in trichomes ($P=0.003$) indicating that *ETC1* acts redundantly with *ETC3*. By contrast, the *etc2 etc3* double mutant exhibited a trichome density similar to that of the *etc3* single mutant. However, a redundant function of *ETC2* with *ETC3* was uncovered in the *etc1 etc2 etc3* triple mutant, in which a significantly higher trichome number was found as compared

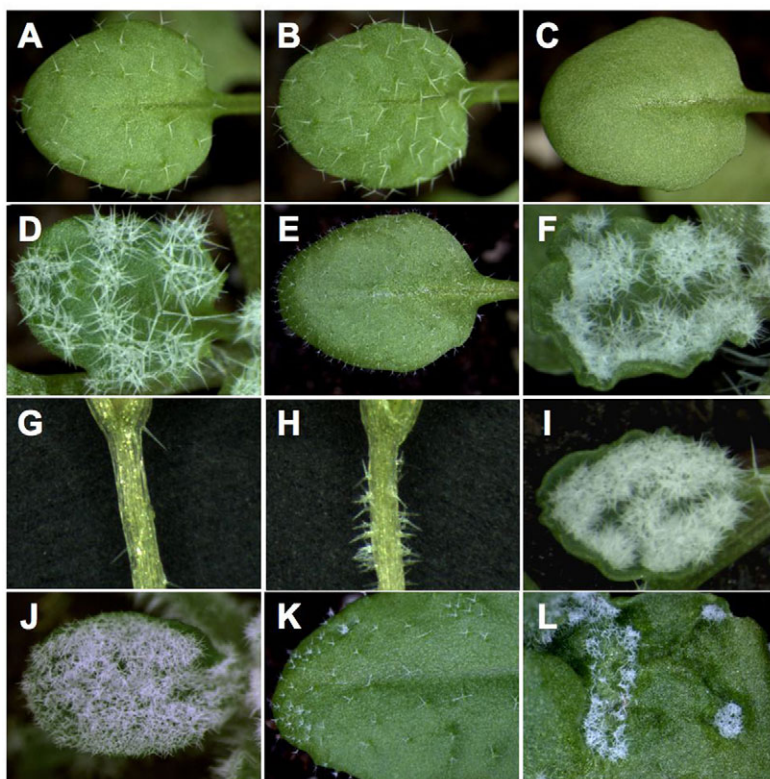


Fig. 2. Phenotypic analysis of trichome formation on rosette leaves in *etc3* single and multiple mutants. (A) Wild-type (Col) *Arabidopsis*. (B) *etc3*. (C) p35S:*ETC3* in a wild-type background. (D) *cpc try*. (E) *etc1 etc2 etc3*. (F) *cpc try etc3*. (G) Hypocotyl of *cpc try*. (H) Hypocotyl of *cpc try etc3*. (I) *cpc try etc1 etc2*. (J) *cpc try etc1 etc3*. (K) Phenotype of *cpc try etc3* mutant plants rescued by pTRY:*ETC3*. (L) Phenotype of *cpc try etc3* mutant plants rescued by pCPC:*ETC3*.

Table 2. Trichome numbers in *etc3* double and triple mutants

Genotype	First leaf pair			Second leaf pair			Mean cluster size
	Trichome initiation sites per leaf	Trichomes per leaf	Trichome clusters per leaf (%)	Trichome initiation sites per leaf	Trichomes per leaf	Trichome clusters per leaf (%)	
WT (Col)	16.6±2.2	16.6±2.2	0	45.5±7.2	45.5±7.2	0	–
<i>etc3</i> (Col)	25.6±2.9	25.6±2.9	0	71.0±10.4	71.0±10.4	0	–
<i>etc1</i> (Col)	19.9±2.6	19.6±2.6	0	53.1±9.6	53.1±9.6	0	–
<i>try</i> (Col)	16.5±2.3	18.6±2.0	6.2	40.3±6.4	48.9±7.9	10.5	2.0
<i>etc3 try</i>	24.7±3.3	28.8±4.5	8.4	53.5±7.1	66.7±8.9	11.9	2.1
<i>etc3 etc1</i>	36.7±4.6	37.1±4.6	0.5	88.6±11.4	89.6±11.4	0.5	2.0
WT (WS)	19.8±2.5	19.8±2.5	0	66.7±13.3	66.7±13.3	0	–
<i>cpc</i> (WS)	27.7±3.7	27.7±3.7	0	102.7±16.9	102.8±17.0	0.1	2
<i>etc2</i> (WS)	24.3±2.9	24.3±2.9	0	75.0±12.8	75.0±12.8	0	–
<i>etc3 etc2</i>	30.5±3.5	30.5±3.5	0	78.9±11.9	78.9±11.9	0	–
<i>etc3 cpc</i>	38.8±3.9	39.2±3.9	0.6	106.8±17.9	107.1±18.1	0.1	2.0
<i>etc1 etc2</i>	47.0±3.0	47.0±3.0	0	136.2±11.1	136.2±11.1	0	–
<i>etc1 etc2 etc3</i>	92.6±2.5	92.6±2.5	0	>170±n.d.	>170±n.d.	0	–

At least 20 plants for each line were used for the analysis.

WT, wild type; n.d., not determined.

with the *etc1 etc3* double mutant (Fig. 2E; Table 2). A much stronger effect was found in the *etc3 try cpc* triple mutant, in which only a few large clusters of trichomes were found that contained more than 100 trichomes (Fig. 2F). A phenotypic enhancement was also observed for ectopic trichome formation on the hypocotyl (Fig. 2G,H). The phenotypic strength of this triple mutant was increased in the *etc1 etc3 try cpc* (Fig. 2J) and *etc1 etc2 try cpc* (Fig. 2I) quadruple mutants.

Role of *ETC3* in root hair and stomata development

Tominaga and co-workers noted a reduction of root hairs in the *etc3* single mutant (Tominaga et al., 2008), whereas Wang and co-workers did not (Wang et al., 2008).

We analysed the root hair pattern with respect to the underlying cortex cells (Table 3), focusing on the *etc3* mutant and *cpc etc3* double mutant. In *etc3* mutants the number of root hairs in trichoblast positions was significantly decreased ($P<0.01$). The *cpc etc3* double mutant showed no difference compared with *cpc*, and the overexpression line p35S:ETC3 exhibited significantly more root hairs in the atrichoblast position ($P<0.01$) (Table 3).

Because of the strong and specific expression of *ETC3* in stomata (Fig. 1E) we also analysed the stomata pattern in the leaf epidermis of *etc3* mutants and in p35S:ETC3 lines. In addition, we tested the double mutant *etc3 etc2* because *ETC2* is the only other gene of the *TRY/CPC* group that shows strong expression in stomata. As reported by Tominaga and co-workers (Tominaga et al., 2008), we found no deviation from wild type in any of these lines (data not shown).

ETC3 phenotypes unrelated to canonical *TRY/CPC* functions

Tominaga and co-workers reported several *etc3* mutant phenotypes that are not observed for any of the other *TRY/CPC* group mutants. These include an early flowering phenotype under long-day conditions, a reduction of trichome size and branching, an increase in hypocotyl length, and drastic overall growth changes. Our combination of a null mutant and a genomic rescue of this mutant enabled us to reassess these unusual phenotypes.

The flowering time was studied under long-day conditions (16 hours light/8 hours dark) (see Table S1 in the supplementary material). Under these conditions, wild-type plants flowered after 27±1 days ($n=20$), whereas *etc3* mutants flowered after 28±1 days ($n=20$). By that time, wild-type and *etc3* plants had produced 13±1 and 15±1 rosette leaves, respectively. The same behaviour was found for plants kept under continuous light conditions. An early flowering phenotype was not observed.

In our hands, trichome size was indistinguishable in wild type and *etc3* mutants (see Fig. S2 in the supplementary material). The marked reduction reported by Tominaga and co-workers (Tominaga et al., 2008) was not observed. Also, trichome branching was not affected in the *etc3* mutant (see Table S2 in the supplementary material).

Hypocotyls were reported to almost double in length in *etc3* mutants and to be shorter in 35S:ETC3 plants, which was correlated with changes in the epidermal cell shape (Tominaga et al., 2008). We could not detect any difference in hypocotyl length between wild type, *etc3* and 35S:ETC3 mutants (see Fig. S3 in the supplementary material), nor any epidermal cell shape changes (data not shown).

Table 3. Root hair formation in the root epidermis of *etc3* mutants and *ETC3* overexpression lines

Genotype	Hair cells in epidermis (%)	Trichoblast position		Atrichoblast position	
		Hair cells (%)	Non-hair cells (%)	Hair cells (%)	Non-hair cells (%)
WT (Col)	41.2±1.7	93.5±9.6	6.5±9.6	8.9±9.9	91.1±9.9
WT (WS)	40.1±3.8	90.7±9.0	9.3±9.0	2.1±4.8	97.9±4.8
<i>etc3</i> (Col)	27.3±1.5	73.9±15.9	26.1±15.9	1.1±3.6	98.9±3.6
<i>cpc</i> (WS)	11.8±1.7	16.2±11.1	83.8±11.1	0±0	100±0
<i>etc3 cpc</i>	9.6±1.4	15.7±11.1	84.3±11.1	0±0	100±0
p35S:ETC3	62.0±4.5	100±0	0±0	36.1±13.3	63.9±13.3

Five-day-old seedlings grown on MS plates were used. At least 20 roots were studied for each line.

WT, wild type.

When comparing overall plant growth we noted moderate differences between wild-type, *etc3*, 35S:ETC3 and pETC3:ETC3 plants with respect to rosette leaf size and height (see Fig. S4 in the supplementary material).

Together, these data suggest that most non-canonical phenotypes previously reported for the *etc3* mutant are not caused by the mutation in the *ETC3* gene.

Expression of ETC3 protein under the *TRY* or *CPC* promoter can rescue *etc3* mutants

The overlapping redundancy of the five *TRY/CPC* genes raises the question of whether the relative differences in their importance for trichome patterning are due to differences in the regulation of their expression or in protein function. As a first step, we compared the ability of *ETC3* to rescue the *etc3* mutant under its own promoter, the *TRY* promoter and the *CPC* promoter. All rescue experiments described here were analysed in the first generation progeny (T1) using 45 plants. The three constructs rescued the *etc3* phenotype equally well (Table 1). This indicates that the *TRY*, *CPC* and *ETC3* promoters are interchangeable with respect to *etc3* rescue.

This result prompted us to consider to what extent the expression of *ETC3* under these three promoters can rescue the *cpc try etc3* triple mutant. To our surprise, we found qualitatively different results for the three constructs. As expected, the pETC3:ETC3 construct rescued the *cpc try etc3* mutant to the same extent as the *try cpc* mutant. When using the pTRY:ETC3 and pCPC:ETC3 constructs, we observed a wide range of rescue phenotypes and often plants were rescued back to the *try cpc* phenotype or even exhibited an over-rescued phenotype resembling that of *try*. The over-rescue phenotype was never observed in pETC3:ETC3 lines. We noted one striking difference between pTRY:ETC3 and pCPC:ETC3 with respect to the intermediate phenotypes. In pTRY:ETC3 we observed huge, separated trichome clusters that were typically devoid of trichomes in their middle region (Fig. 2K). The pCPC:ETC3 construct, by contrast, showed only a few clusters and these were smaller than in the *try cpc* mutants and trichomes were arranged irregularly at a high density (Fig. 2L). Although we do not understand the exact basis for these different patterns, these results strongly suggest that the qualitatively different phenotypes of *try* and *cpc* are due to differences in the regulation of their expression.

Localisation and cell-to-cell movement of ETC3

The localisation of the ETC3 protein was initially determined using a p35S:YFP-ETC3 construct. As shown in Fig. 3A, the protein was localised in the nucleus as well as in the cytoplasm. Expression under the control of its own promoter revealed a more differentiated pattern. We compared the expression and localisation of two constructs. The pETC3:GFP-ER construct was used as a control to visualise the expression pattern with a non-mobile GFP protein. In pETC3:GFP-ER lines, expression was only found in single cells (Fig. 3C). The ubiquitous expression detected with the GUS lines was not observed, most likely because the sensitivity of the GFP signal was much lower than in the GUS lines. In pETC3:YFP-ETC3 lines, by contrast, cells around an incipient trichome showed a clear YFP signal. Strikingly, the YFP-ETC3 signal in surrounding cells was restricted to the nucleus, whereas in trichome initials YFP-ETC3 was found both in the cytoplasm and in the nucleus (Fig. 3B). This indicates that ETC3 protein moves from the trichome initial into the neighbouring epidermal cells.

We also demonstrated movement of ETC3 in two independent experiments. First, by expressing ETC3 in the subepidermis under the control of the *RUBISCO* promoter, in the construct pRbc:YFP-ETC3,

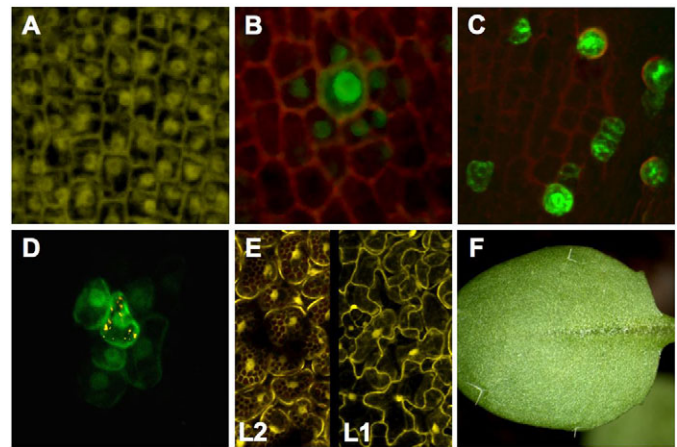


Fig. 3. Localisation and movement of ETC3 protein. (A–D) Confocal laser-scanning microscopy (CLSM) of sections of the basal part of young rosette leaves in wild-type (Col) *Arabidopsis* plants. Cell walls in B and C are labeled in red by propidium iodide and the localisation of YFP-tagged ETC3 is in green. (A) p35S:YFP-ETC3. (B) pETC3:YFP-ETC3. Note that the trichomes and immediate neighbours show fluorescence. (C) pETC3:GFP-ER. Note that the cell-autonomous GFP-ER is restricted to trichome initials and is not found in the neighbours at the same developmental stages. (D) Transient expression of p35S:GFP-ETC3 by particle bombardment. p35S:YFP-PTS (yellow) marks the transformed cell. (E) Subepidermal expression of pRbc:YFP-ETC3 in rosette leaf (CLSM). The left-hand picture (L2) shows a subepidermal section. Chloroplasts are red owing to auto-fluorescence. The right-hand picture (L1) shows an epidermal section. (F) Trichome suppression in a wild-type background mediated by subepidermal expression of pRbc:YFP-ETC3.

in a wild-type background. If ETC3 were able to move into the epidermis one would expect a trichome reduction similar to that found in p35S:ETC3 lines. In these lines, a clear reduction of trichomes was observed (Fig. 3F; Table 1). Direct microscopic inspection revealed fluorescence in the epidermis suggesting that YFP-ETC3 protein or RNA has moved into the epidermis (Fig. 3E,F).

In a second experiment, p35S:GFP-ETC3 was transiently expressed in single leaf epidermal cells using the particle bombardment method. As shown in Fig. 3D, fluorescence was also found in cells around the cell expressing the construct. This movement was observed in 76% of all successfully transformed cells ($n=100$).

Protein-protein interactions of ETC3

The most important recognised protein-protein interaction of TRY and CPC during pattern formation is their binding to GL3. As shown in Fig. 4A, all five TRY/CPC group proteins showed strong binding to GL3 in yeast two-hybrid assays. This interaction was confirmed for TRY, CPC, ETC1, ETC2 and ETC3 with the BiFC system (Fig. 4B). As a control we used the truncated GL3 protein lacking the N-terminal 96 amino acids that was previously shown not to bind to GL1, TRY, CPC, ETC1, ETC2 or ETC3 in yeast two-hybrid assays (Kirik et al., 2005; Payne et al., 2000) (data not shown). The interaction of the TRY/CPC proteins with GL3 competes with the interaction of GL1 with GL3. We used this situation to study whether the TRY/CPC group proteins compete with GL1 with different efficiency using the yeast three-hybrid system. Growth at different concentrations of methionine was compared (Fig. 4C–F). At 500 μ M methionine the methionine promoter is inactive (Fig. 4F). At 250 μ M methionine CPC (4*) prevented GL1-GL3

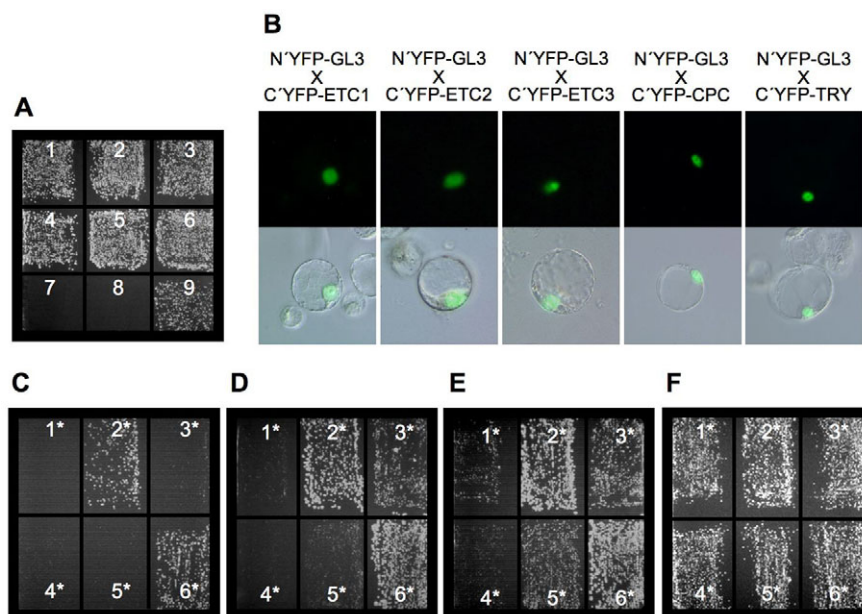


Fig. 4. Protein-protein interaction of ETC3 and its homologues with GL3. (A) Yeast two-hybrid assays with AD-GL3 and BD-ETC1 (1), AD-GL3 and BD-ETC2 (2), AD-GL3 and BD-ETC3 (3), AD-GL3 and BD-CPC (4), AD-GL3 and BD-TRY (5), AD-GL3 and BD-GL1Δ (6), AD-GL3 and pAS vector without fused protein (7), pAct vector without fused protein and pAS vector without fused protein (8), AD-SnF4 and BD-SnF1 (9). Growth indicates interaction between the respective proteins. (B) BiFC in protoplasts of GL3 with ETC1, ETC2, ETC3, CPC or TRY. Upper row, fluorescence micrographs; the lower row is an overlay of the fluorescence micrograph and the corresponding light micrograph. (C-F) Yeast three-hybrid assays. The competition between GL1 and ETC1 (1*), GL1 and ETC2 (2*), GL1 and ETC3 (3*), GL1 and CPC (4*), GL1 and TRY (5*) for binding to GL3 (fused to the GAL4 DNA-AD) is shown. The methionine-repressible promoter in the pBridge vector controls the expression of one of the *CPC/TRY*-like genes in the presence of GL1 (fused to GAL4 DNA-BD). (6*) The two-hybrid interaction between GL3 and GL1 in the absence of ETC3 or its homologues. (C) The interaction plate contains 0 μM methionine. No growth indicates a competition between GL1 and the respective protein. (D-F) The interaction plate contains 100 (D), 250 (E) or 500 (F) μM methionine. The methionine-sensitive promoter is inactive at 500 μM methionine and growth indicates an interaction between GL3 and GL1.

interaction and ETC1 (1*) caused a clear growth reduction (Fig. 4E). At 100 μM methionine TRY (5*) prevented the GL1-GL3 interaction (Fig. 4D), and without methionine ETC3 (3*) could repress growth. ETC2 (2*) showed only a little growth reduction (Fig. 4C). Together, these data suggest that CPC is the most potent competitor followed by ETC1, TRY, ETC3 and ETC2.

As differences in the competition with the GL1-GL3 interaction reflect different binding affinities to GL3 we speculated that this might also affect the movement of the inhibitors. We took a theoretical approach to assess whether this idea is correct. We simulated a situation in which the inhibitor is produced locally and diffuses into the tissue. Along its path, the inhibitor is degraded at a constant rate. In addition, it is depleted owing to binding to GL3 with different binding affinities. We measured the movement ability of the inhibitor by its characteristic decay length (CDL), α , which is the distance over which the level of the inhibitor drops to $1/e$ (37%) of its source level. As shown in Fig. 5, a clear reduction in the movement ability of the inhibitor is predicted for increasing binding affinities. For example, if the relative binding affinity, γ , of the inhibitor of GL3 is increased from 1 to 10, its decay length is decreased from 71% to 30% relative to its CDL in the absence of any binding to GL3. Therefore, a strong binding affinity for GL3 is expected to result in a less mobile inhibitor, whereas a weak binding affinity should make the inhibitor more mobile as long as all other parameters are constant.

To experimentally test the prediction that higher binding affinity for GL3 decreases mobility, we compared the movement behaviour between single cells expressing YFP-CPC and YFP-ETC3 and their

immediate neighbouring cells. In a first series of experiments we co-bombarded YFP-CPC or YFP-ETC3 with the peroxisome marker PTS in order to recognise the transformed cells. To evaluate the influence of GL3 on the movement behaviour we compared movement on rosette leaves of *gl3 egl3* double mutants and a p35S:GL3-overexpression line (Table 4). Movement into neighbouring cells was detected in 74% and 66% of the targeted cells for YFP-ETC3 and YFP-CPC, respectively. Elevated GL3 levels significantly reduced the number of cells from which movement was observed. YFP-CPC movement was reduced to 22%, which corresponds to a reduction to 33% of the levels found in *gl3 egl3* plants. As theoretically expected, YFP-ETC3 movement was much less affected by higher GL3 levels: 39% of the cells still showed movement, which corresponds to 53% of the levels found in *gl3 egl3* plants.

In order to quantify the movement of YFP-CPC and YFP-ETC3 more directly, we measured the fluorescence intensity in the nuclei of the initially transformed cell (source, considered 100%) and the neighbouring cell (target). Again, the p35S:GL3 and *gl3 egl3* plants were used for comparison. As a control we used YFP alone to

Table 4. Frequency of CPC and ETC3 movement into neighbouring cells

Construct	Movement in <i>gl3 egl3</i> (%)	Movement in p35S:GL3 (%)
p35S:YFP-ETC3	74	39
p35S:YFP-CPC	66	22

Movement was analysed for 50 transformed cells on cotyledons.

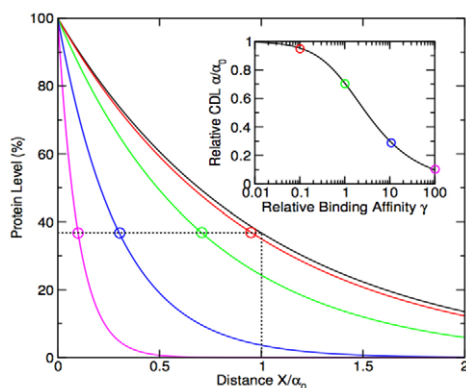


Fig. 5. Modelling of the effect of protein depletion on the mobility of inhibitors. Decay of inhibitor concentration with distance from the source for inhibitors with different binding affinities for GL3. The movement ability of the inhibitor is measured by the characteristic decay length (CDL), α , which is the distance from the source at which the protein level drops to $1/e$ (37%) of its source level. All length scales are relative to α_0 , which is the CDL in the absence of protein binding (dashed line, black curve). Colour coding: absence of protein binding (black), relative binding affinity $\gamma=0.1$ (red), $\gamma=1$ (green), $\gamma=10$ (blue), $\gamma=100$ (magenta). The inset shows the dependence of the CDL on the relative binding affinity, γ . Note the correspondingly coloured circles in the inset and the main graph. As the relative binding affinity of the inhibitor for the activator increases, its CDL decreases (see Materials and methods).

demonstrate that the two mutant backgrounds showed no general differences with respect to protein mobility (Table 5) (Student's t -test, $P=0.315$). In this system we detected a subtle but significant difference between p35S:GL3 and *gl3 egl3* plants for YFP-ETC3 movement (Table 5) (Student's t -test, $P<0.009$). By contrast, the mobility of YFP-CPC was drastically reduced by $\sim 50\%$ in p35S:GL3 plants as compared with *gl3 egl3* plants (Table 5) (Student's t -test, $P=0.000$). The different movement behaviour of CPC and ETC3 in the two mutants was evident from the fact that neither showed a significantly different target/source ratio in *gl3 egl3* mutants (Table 5) (Student's t -test, $P=0.129$), but highly significant differences in p35S:GL3 plants (Table 5) (Student's t -test, $P=0.000$). The robustness of all Student's t -test results was confirmed using a non-parametric test according to Mann-Whitney (U -test). Together, the data indicate that the presence of GL3 reduces CPC mobility more efficiently than it reduces ETC3 mobility.

DISCUSSION

The presence of six close homologues of the R3 MYB transcription factor family and their involvement in root hair and trichome development raises two major questions. First, what is their relative contribution in the two processes and second, how are different functional adaptations realised?

Functional diversity of R3 MYB transcription factors

Phylogenetic analysis groups *TRY* and *ETC2* in one tree and *CPC*, *TCL1*, *ETC1* and *ETC3* in a second tree (Wang et al., 2007); within this tree, *CPC* is separated from *TCL1* and a second branch containing *ETC1* and *ETC3*. How does this evolutionary tree fit with their functional adaptations in root hair development and trichome formation?

Table 5. Nuclear signal ratio of YFP, YFP-CPC and YFP-ETC3 of neighbouring (target) to transiently transformed (source) cells

Construct	Target/source ratio (%)	
	<i>gl3 egl3</i>	p35S:GL3
p35S:YFP-ETC3*	44.0 \pm 13.1	36.2 \pm 7.0
p35S:YFP-CPC*	39.2 \pm 8.8	20.7 \pm 4.9
p35S:YFP [†]	21.2 \pm 4.4	22.0 \pm 3.6

* $n=23$.

[†] $n=15$.

Five of the six R3 MYB genes are involved in the regulation of root hair formation, although to different extents. *CPC* has the most prominent role and the corresponding mutants show a strong reduction of root hairs (Wada et al., 1997). A function for *TRY* and *ETC1* was recognised in the respective double mutants with *cpc*; the *try* and *etc1* single mutants are indistinguishable from wild type (Kirik et al., 2004a; Schellmann et al., 2002). A function of *TCL1* in root hair formation was recognised in a *cpc etc1 etc3 tcl1* mutant (Wang et al., 2008). A role of *ETC3* in root hair formation was suggested by Tominaga et al. (Tominaga et al., 2008) and by our data presented here. However, such a role was not found in two previous studies (Simon et al., 2007; Wang et al., 2008), which might be explained by different growth conditions.

By contrast, all six R3 MYB genes play a role in trichome formation. This, however, does not simply constitute redundant action, as found for *ETC1*, but also functional diversification. *TRY* seems to be important for the local selection of trichome cells as suggested by a cluster phenotype in *try* mutants (Hulskamp et al., 1994). *CPC*, *ETC2* and *ETC3* seem to regulate the distance between trichomes as indicated by a higher trichome density in these mutants (Kirik et al., 2004b; Schellmann et al., 2002). Finally, *TCL1* is important for organ-specific trichome regulation (Wang et al., 2007), although a role in pattern formation on leaves is also suggested by the *tcl1 cpc etc1 etc3* phenotype (Wang et al., 2008). The double and triple mutant analyses revealed plenty of redundancies between these three regulatory aspects. The *etc3 try* and *etc2 try* double mutants, for example, revealed an additional function of *ETC3* and *ETC2* in the local selection process (Kirik et al., 2004b). The triple mutant combination of *etc1* and *etc2* with the *try cpc* double mutant revealed a region specificity for *ETC1* and *ETC2* in the regulation of the trichome formation of petioles (Kirik et al., 2004a; Kirik et al., 2004b). Conversely, the synergistic enhancement of trichome formation on pedicels and stem in the *tcl1 cpc* double mutants indicates a redundancy between *TCL1* and *CPC* (Wang et al., 2007). Taken together, there is no obvious correlation between the functional diversification and evolutionary distances of these proteins.

Expression or protein function: which is relevant for functional diversification?

Differences in transcriptional regulation are the most obvious reason for functional diversification. This is particularly evident for *ETC2* and *TCL1*, neither of which is expressed in the root (Kirik et al., 2004b; Wang et al., 2007). In all other cases, the expression pattern is almost indistinguishable in root and shoot. The expression levels seem to vary in RT-PCR experiments; however, it is not possible to judge the relevance of this as the expression levels in the relevant cell types (trichoblast or atrichoblast/trichomes or epidermal cells) at the time when the pattern is established remain elusive. Also, our promoter-swap experiments suggest relevant differences at the promoter level, as *etc3 try cpc* triple mutants can be over-rescued when *ETC3* is expressed under control of the *CPC* or *TRY* promoter.

Promoter-swap experiments also revealed examples demonstrating differences at the protein level. In the root system the rescue of the *cpc* mutant phenotype with *CPC*-promoter driven cDNAs of the R3 MYB family revealed clear differences, such that *ETC1* rescued best, followed by *ETC3*, *TRY* and *ETC2* (Simon et al., 2007). In the same experimental set-up, the *cpc* trichome phenotype was rescued equally well by all proteins except for *TRY*, which over-rescued. *TCL1* seems to have diverged the most among the R3 MYB group at the protein level. Whereas overexpression of all the other genes causes supernumerary root hairs, *TCL1* overexpression has no effect on root hair formation (Wang et al., 2007). A difference is also seen in the trichome system, such that *TCL1* expression under the *CPC* promoter can rescue the *cpc* mutant phenotype but expression under the *TRY* promoter cannot rescue the *try* mutant phenotype (Wang et al., 2007).

Protein properties: which aspects matter for patterning?

Currently, two mechanisms are proposed to explain how the R3 MYB proteins inhibit the activators. First, it is suggested that *TCL1* can bind directly to the regulatory DNA regions thereby repressing their expression (Wang et al., 2007), although no evidence supporting such a mechanism is available for any of the other group members. Second, it is suggested that GL1-GL3 dimerisation is inhibited by binding of the inhibitors to GL3 (Esch et al., 2003). We demonstrated here that this property is shared by *CPC*, *TRY*, *ETC1*, *ETC2* and *ETC3*. It is likely that *TCL1* also shares this function as it can bind to GL3 (Wang et al., 2008).

Our finding that the five analysed inhibitors differed in their ability to interfere with the GL1-GL3 interaction raised the question of whether this might be relevant for their role in patterning. Theoretical models provide the key criteria to formulate the relevant parameters (Koch and Meinhardt, 1994): (1) the binding strength to GL3 or to DNA; (2) the diffusion/transport rates; and (3) the degradation rates. Our theoretical calculations suggest that if all other parameters are constant, movement of the inhibitors should be affected by their different binding strengths to GL3, such that *ETC2* moves best and *CPC* least. Focusing on the movement of YFP-*CPC* and YFP-*ETC3* between two cells, we provide two lines of evidence supporting the theoretical prediction. First, we show that the number of transiently transformed cells from which movement is observed depends on the presence of GL3 and that this affects *CPC* movement more than that of *ETC3*. In a second line of experiments we measured the fraction of YFP-*CPC* or YFP-*ETC3* that had moved into the neighbouring cell, and again *CPC* mobility was increased in the absence of GL3, whereas *ETC3* movement was not. It is important to note that these predictions cannot be simply extended to the whole patterning process and to the phenotypic differences between the mutants because a quantitative determination of the expression levels in trichomes, a quantitative comparison of the protein degradation rates and a quantitative evaluation of the transport rates between the cells are missing. Future steps towards a mechanistic understanding of the patterning systems will require not only an unravelling of the genetic and molecular network, but also a combination of quantitative experimental and theoretical approaches.

Sincere thanks to Victor Kirik for primarily discussions about the *CPC/TRY*-like genes. We thank the David Jackson laboratory for the *RUBISCO SMALL SUBUNIT 2B* promoter; Daniel Bouyer for the *cpc try etc1 etc2* quadruple mutant and the pRbc:pAM-PAT construct; Martina Pesch for the pCPC:pAM-PAT and pTRY:pAM-PAT constructs; Jaideep Mathur for the p35S:YFP-PTS construct; Sean Chapman for the BiFC-compatible pBATL vectors; and the European *Arabidopsis* Stock Centre NASC for the SALK line 094027 (*etc3*).

This work was supported by the SFB 572 and the Graduate School for Biological Sciences at the University of Cologne. F.G. was supported by the FP6 COSBICS Project (512060).

Supplementary material

Supplementary material for this article is available at <http://dev.biologists.org/cgi/content/full/136/9/1487/DC1>

References

- Berger, F., Haseloff, J., Schiefelbein, J. and Dolan, L. (1998). Positional information in root epidermis is defined during embryogenesis and acts in domains with strict boundaries. *Curr. Biol.* **8**, 421-430.
- Bergmann, D. C. and Sack, F. D. (2007). Stomatal development. *Annu. Rev. Plant Biol.* **58**, 163-181.
- Bernhardt, C., Lee, M. M., Gonzalez, A., Zhang, F., Lloyd, A. and Schiefelbein, J. (2003). The bHLH genes *GLABRA3* (*GL3*) and *ENHANCER OF GLABRA3* (*EGL3*) specify epidermal cell fate in the *Arabidopsis* root. *Development* **130**, 6431-6439.
- Bernhardt, C., Zhao, M., Gonzalez, A., Lloyd, A. and Schiefelbein, J. (2005). The bHLH genes *GL3* and *EGL3* participate in an intercellular regulatory circuit that controls cell patterning in the *Arabidopsis* root epidermis. *Development* **132**, 291-298.
- Bouyer, D., Geier, F., Kragler, F., Schnittger, A., Pesch, M., Wester, K., Balkunde, R., Timmer, J., Fleck, C. and Hulskamp, M. (2008). Two-dimensional patterning by a trapping/depletion mechanism: the role of *TTG1* and *GL3* in *Arabidopsis* trichome formation. *PLoS Biol.* **6**, e141.
- Clough, S. and Bent, A. (1998). Floral dip: a simplified method for *Agrobacterium*-mediated transformation of *Arabidopsis thaliana*. *Plant J.* **16**, 735-743.
- Digiuni, S., Schellmann, S., Geier, F., Greese, B., Pesch, M., Wester, K., Dartan, B., Mach, V., Srinivas, B. P., Timmer, J. et al. (2008). A competitive complex formation mechanism underlies trichome patterning on *Arabidopsis* leaves. *Mol. Syst. Biol.* **4**, 217.
- Dolan, L., Duckett, C. M., Grierson, C., Linstead, P., Schneider, K., Lawson, E., Dean, C., Poethig, S. and Roberts, K. (1994). Clonal relationships and cell patterning in the root epidermis of *Arabidopsis*. *Development* **120**, 2465-2474.
- Esch, J. J., Chen, M., Sanders, M., Hillestad, M., Ndkium, S., Idelkope, B., Neizer, J. and Marks, M. D. (2003). A contradictory *GLABRA3* allele helps define gene interactions controlling trichome development in *Arabidopsis*. *Development* **130**, 5885-5894.
- Esch, J. J., Chen, M. A., Hillestad, M. and Marks, M. D. (2004). Comparison of *TRY* and the closely related *At1g01380* gene in controlling *Arabidopsis* trichome patterning. *Plant J.* **40**, 860-869.
- Galway, M. E., Masucci, J. D., Lloyd, A. M., Walbot, V., Davis, R. W. and Schiefelbein, J. W. (1994). The *TTG* gene is required to specify epidermal cell fate and cell patterning in the *Arabidopsis* root. *Dev. Biol.* **166**, 740-754.
- Gietz, R. D. and Schiestl, R. H. (1995). Transforming yeast with DNA. *Methods Mol. Cell Biol.* **5**, 255-269.
- Hulskamp, M. and Schnittger, A. (1998). Spatial regulation of trichome formation in *Arabidopsis thaliana*. *Semin. Cell Dev. Biol.* **9**, 213-220.
- Hulskamp, M., Misera, S. and Jürgens, G. (1994). Genetic dissection of trichome cell development in *Arabidopsis*. *Cell* **76**, 555-566.
- Ishida, T., Kurata, T., Okada, K. and Wada, T. (2008). A genetic regulatory network in the development of trichomes and root hairs. *Annu. Rev. Plant Biol.* **59**, 364-386.
- Kirik, V., Schnittger, A., Radchuk, V., Adler, K., Hulskamp, M. and Baumlein, H. (2001). Ectopic expression of the *Arabidopsis AtMYB23* gene induces differentiation of trichome cells. *Dev. Biol.* **235**, 366-377.
- Kirik, V., Simon, M., Hulskamp, M. and Schiefelbein, J. (2004a). The *ENHANCER OF TRY* and *CPC1* (*ETC1*) gene acts redundantly with *TRIPTYCHON* and *CAPRICE* in trichome and root hair cell patterning in *Arabidopsis*. *Dev. Biol.* **268**, 506-513.
- Kirik, V., Simon, M., Wester, K., Schiefelbein, J. and Hulskamp, M. (2004b). *ENHANCER OF TRY* and *CPC 2* (*ETC2*) reveals redundancy in the region-specific control of trichome development of *Arabidopsis*. *Plant Mol. Biol.* **55**, 389-398.
- Kirik, V., Lee, M. M., Wester, K., Herrmann, U., Zheng, Z., Oppenheimer, D., Schiefelbein, J. and Hulskamp, M. (2005). Functional diversification of *MYB23* and *GL1* genes in trichome morphogenesis and initiation. *Development* **132**, 1477-1485.
- Koch, A. J. and Meinhardt, H. (1994). Biological pattern formation: from basic mechanisms to complex structures. *Rev. Mod. Phys.* **66**, 1481-1507.
- Larkin, J. C., Young, N., Prigge, M. and Marks, M. D. (1996). The control of trichome spacing and number in *Arabidopsis*. *Development* **122**, 997-1005.
- Larkin, J. C., Walker, J. D., Bolognesi-Winfield, A. C., Gray, J. C. and Walker, A. R. (1999). Allele-specific interactions between *ttg* and *gl1* during trichome development in *Arabidopsis thaliana*. *Genetics* **151**, 1591-1604.
- Larkin, J. C., Brown, M. L. and Schiefelbein, J. (2003). How do cells know what they want to be when they grow up? Lessons from epidermal patterning in *Arabidopsis*. *Annu. Rev. Plant Biol.* **54**, 403-430.

- Lee, M. M. and Schiefelbein, J. (1999). WEREWOLF, a MYB-related protein in Arabidopsis, is a position-dependent regulator of epidermal cell patterning. *Cell* **99**, 473-483.
- Marks, M. D. and Esch, J. J. (2003). Initiating inhibition: control of epidermal cell patterning in plants. *EMBO Rep.* **4**, 24-25.
- Mathur, J., Mathur, N. and Hulskamp, M. (2002). Simultaneous visualization of peroxisomes and cytoskeletal elements reveals actin and not microtubule-based peroxisome motility in plants. *Plant Physiol.* **128**, 1031-1045.
- Oppenheimer, D. G., Herman, P. L., Sivakumaran, S., Esch, J. and Marks, M. D. (1991). A myb gene required for leaf trichome differentiation in Arabidopsis is expressed in stipules. *Cell* **67**, 483-493.
- Payne, C. T., Zhang, F. and Lloyd, A. M. (2000). GL3 encodes a bHLH protein that regulates trichome development in Arabidopsis through interaction with GL1 and TTG1. *Genetics* **156**, 1349-1362.
- Pesch, M. and Hulskamp, M. (2004). Creating a two-dimensional pattern de novo during Arabidopsis trichome and root hair initiation. *Curr. Opin. Genet. Dev.* **14**, 422-427.
- Schellmann, S., Schnittger, A., Kirik, V., Wada, T., Okada, K., Beermann, A., Thumfahrt, J., Jurgens, G. and Hulskamp, M. (2002). TRIPTYCHON and CAPRICE mediate lateral inhibition during trichome and root hair patterning in Arabidopsis. *EMBO J.* **21**, 5036-5046.
- Schellmann, S., Hulskamp, M. and Uhrig, J. (2007). Epidermal pattern formation in the root and shoot of Arabidopsis. *Biochem. Soc. Trans.* **35**, 146-148.
- Scheres, B. (2002). Plant patterning: TRY to inhibit your neighbors. *Curr. Biol.* **12**, R804-R806.
- Serna, L. (2005). Epidermal cell patterning and differentiation throughout the apical-basal axis of the seedling. *J. Exp. Bot.* **56**, 1983-1989.
- Simon, M., Lee, M. M., Lin, Y., Gish, L. and Schiefelbein, J. (2007). Distinct and overlapping roles of single-repeat MYB genes in root epidermal patterning. *Dev. Biol.* **311**, 566-578.
- Spitzer, C., Schellmann, S., Sabovljevic, A., Shahriari, M., Keshavaiah, C., Bechtold, N., Herzog, M., Muller, S., Hanisch, F. G. and Hulskamp, M. (2006). The Arabidopsis elch mutant reveals functions of an ESCRT component in cytokinesis. *Development* **133**, 4679-4689.
- Tominaga, R., Iwata, M., Sano, R., Inoue, K., Okada, K. and Wada, T. (2008). Arabidopsis CAPRICE-LIKE MYB 3 (CPL3) controls endoreduplication and flowering development in addition to trichome and root hair formation. *Development* **135**, 1335-1345.
- Vroemen, C. W., Langeveld, S., Mayer, U., Ripper, G., Jurgens, G., Van Kammen, A. and De Vries, S. C. (1996). Pattern formation in the Arabidopsis embryo revealed by position-specific lipid transfer protein gene expression. *Plant Cell* **8**, 783-791.
- Wada, T., Tachibana, T., Shimura, Y. and Okada, K. (1997). Epidermal cell differentiation in Arabidopsis determined by a Myb homolog, CPC. *Science* **277**, 1113-1116.
- Walker, A. R., Davison, P. A., Bolognesi-Winfield, A. C., James, C. M., Srinivasan, N., Blundell, T. L., Esch, J. J., Marks, M. D. and Gray, J. C. (1999). The TRANSPARENT TESTA GLABRA1 locus, which regulates trichome differentiation and anthocyanin biosynthesis in Arabidopsis, encodes a WD40 repeat protein. *Plant Cell* **11**, 1337-1349.
- Wang, S., Kwak, S. H., Zeng, Q., Ellis, B. E., Chen, X. Y., Schiefelbein, J. and Chen, J. G. (2007). TRICHOMELESS1 regulates trichome patterning by suppressing GLABRA1 in Arabidopsis. *Development* **134**, 3873-3882.
- Wang, S., Hubbard, L., Chang, Y., Guo, J., Schiefelbein, J. and Chen, J. G. (2008). Comprehensive analysis of single-repeat R3 MYB proteins in epidermal cell patterning and their transcriptional regulation in Arabidopsis. *BMC Plant Biol.* **8**, 81.
- Zhang, F., Gonzalez, A., Zhao, M., Payne, C. T. and Lloyd, A. (2003). A network of redundant bHLH proteins functions in all TTG1-dependent pathways of Arabidopsis. *Development* **130**, 4859-4869.